ELSEVIER

Sensitivity of regional climate to deforestation in the Amazon basin

Elfatih A. B. Eltahir & Rafael L. Bras

Ralph M. Parsons Laboratory, Department of Civil and Environmental Engineering, Massachusetts Institute of Technology, Cambridge, Massachusetts 02139-4307, USA

Deforestation results in several adverse effects on the natural environment. The focus of this paper is on the effects of deforestation on land-surface processes and regional climate of the Amazon basin. In general, the effects of deforestation on climate are likely to depend on the scale of the deforested area. In this study, we are interested in the effects due to deforestation of areas with a scale of about 250 km. Hence, a meso-scale climate model is used in performing numerical experiments on the sensitivity of regional climate to deforestation of areas with that size. It is found that deforestation results in less net surface radiation, less evaporation, less rainfall, and warmer surface temperature. The magnitude of the change in temperature is of the order of 0·5°C, the magnitudes of the changes in the other variables are of the order of 10%.

In order to verify some of the results of the numerical experiments, the model simulations of net surface radiation are compared to recent observations of net radiation over cleared and undisturbed forest in the Amazon. The results of the model and the observations agree in the following conclusion: the difference in net surface radiation between cleared and undisturbed forest is, almost, equally partitioned between net solar radiation and net long-wave radiation. This finding contributes to our understanding of the basic physics in the deforestation problem.

1 INTRODUCTION

In the last few decades, the rain-forest of the Amazon has been replaced with short grass over large areas. Figure 1[21] shows estimates of the total deforested area in Brazilian Amazonia. According to these estimates, the deforestation rate in that region is of the order of $2 \times 10^4 \text{ km}^2$ per year. Deforestation is not restricted to the Amazon region; it occurs over other regions of the tropics. Such large-scale human activity is likely to result in serious impacts on the natural environment.

Tropical deforestation results in several adverse effects on the environment. These effects are likely to cover a wide range of scales including global, regional and local. For example, it is estimated that tropical deforestation contributes significantly to the global anthropogenic emissions of CO_2, see Houghton.[17] In addition, recent observations from the Amazon region indicate that burning of the forests is accompanied by release of radiatively active trace gases such as ozone and methane, see Harris *et al.*[16] The increases in anthropogenic emissions of all these gases suggest that tropical deforestation contributes significantly to the global warming problem. On the other hand,

deforestation changes some important land-surface properties; it modifies the surface energy balance and affects hydrologic processes such as evaporation. These changes in surface processes may result in important climate changes at the local and regional scales.

The concern about the possible climatic effects of deforestation has prompted many studies investigating the effects of deforestation on land-surface processes and regional climate. These studies attempted to assess the sensitivity of regional climate in the Amazon basin to deforestation using General Circulation Models (GCMs). The results of the modeling studies, e.g. Lean and Warrilow[19] and Nobre *et al.*[21] predict that large-scale deforestation (~ 2500 km) in the Amazon basin is likely to result in the following changes: less evaporation, less rainfall, and warmer surface temperature. The magnitudes of the changes in evaporation and rainfall are of the order of 20 to 30%, the magnitude of the change in surface temperature is of the order of 2°C.

The studies mentioned above focused on the possible effects due to deforestation of very large areas in the Amazon. It is usually assumed that the deforested area is roughly equivalent to the total area of the Amazon basin which is of the order of $6 \times 10^6 \text{ km}^2$. As shown in
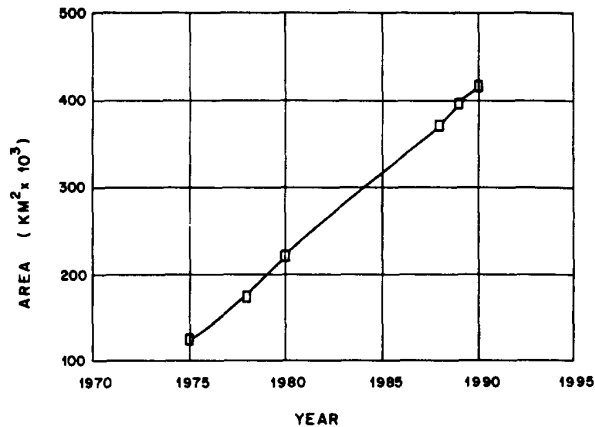
Fig. 1. Total deforested area in Brazilian Amazonia.[21] (Reproduced with permission from the American Meteorological Society.)

Fig. 1, the total deforested area observed in Brazilian Amazonia is about $5 \times 10^5 \, km^2$. Since this total area is distributed over several locations, it is likely that the size of any single deforested area in the region would be approximately $10^4 \, km^2$ or smaller. Hence, although deforestation of the total area of the rain-forest in the Amazon represents the worst possible scenario, the size of that area is signficantly larger than the size of any single deforested area which currently exists in the Amazon region. This study focuses on the climatic effects due to deforestation of a single area of about $6 \times 10^4 \, km^2$. The corresponding linear scale of interest is 250 km which is one order of magnitude smaller than the linear scale of the Amazon basin ($\sim 2500 \, km$).

The approach followed in this study is to use a numerical meso-scale model of the land–atmosphere system to conduct sensitivity experiments on the climate of the Amazon region. The model is driven by solar radiation and boundary conditions from assimilated data. The sensitivity experiment consists of two climate simulations: a pre-deforestation simulation (control), and a post-deforestation simulation (perturbed). The effects of deforestation on the model climate are estimated by the differences between the control and the perturbed climate. Two months, January and July, are chosen for these experiments as they represent typical summer and winter conditions, respectively.

During the last few years, several field experiments were conducted in the Amazon region to collect data on micrometeorology of the rain-forest and the cleared areas, see Shuttleworth,[24] Shuttleworth et al.[26] and Bastable et al.[5] These experiments provide the first observations on the climatic effects of deforestation in the Amazon region. Some of these observations are suitable for comparison with the results of the numerical experiments on the deforestation problem. In this paper, we will compare some aspects of the results of our numerical experiments to the observations from the field experiments.

The paper is organized into five sections. Section 2 describes the climate model which is used in this study, Section 3 describes the design and results of the sensitivity experiments, Section 4 reviews some of the results of the field experiments and compares them to the results of the numerical experiments and Section 5 includes discussion and conclusions of the study.

2 DESCRIPTION OF THE CLIMATE MODEL

This section describes the climate model which is used in the sensitivity experiments. The original version of the model is the Pennsylvania State University/National Center for Atmospheric Research (PSU/NCAR) model. It is also referred to as the Meso-scale Model version 4 (MM4). It was originally developed for meso-scale meteorological studies. The model which is used in this study is an augmented version of MM4; it has been modified to suit climate studies, see Giorgi.[14] The land-surface hydrology scheme is the Biosphere–Atmosphere Transfer Scheme (BATS). In this study, BATS is modified to improve on the hydrology of the scheme.

2.1 The MM4 for meteorological studies

MM4 is a compressible and hydrostatic model which solves the primitive equations in a terrain varying vertical coordinate. The model is driven by boundary conditions and solar radiation. It includes the bulk boundary layer parametrization of Deardorff[6] and the cumulus parametrization of Anthes,[1] which is of the Kuo type. MM4 includes a simple long-wave radiative cooling scheme. The basic structure of the MM4 is described by Anthes et al.[3] The MM4 has been used successfully in a large number of meteorological studies, see Anthes[2] for a review of these studies.

2.2 The MM4 for climate studies

For climate studies, it is necessary to use accurate descriptions of radiative transfer in the atmosphere and near the surface. The augmented version of MM4 has the same structure as the original MM4 except that it includes a sophisticated surface physics and soil hydrology package, an explicit boundary layer formulation, and a more detailed treatment of radiative transfer.

The surface physics and soil hydrology package is BATS, introduced by Dickinson et al.[8] It will be described in some detail in the next section. The radiation parametrization is the same scheme as the one used by the NCAR GCM. It performs separate calculations of atmospheric heating rates and surface fluxes for solar and infrared radiation for clear and cloudy skies. The solar clear sky scheme follows the parametrization of Lacis and Hansen.[18] The solar

cloudy sky scheme accounts for reflection at the top of the clouds, multiple reflections between the clouds, and between the ground and clouds. Infrared radiative transfer scheme includes the contribution of atmospheric gases and clouds.

Two recent studies, Anthes et al.[4] and Giorgi and Bates,[15] focus on the climatological ability of MM4. They test the ability of the model in simulating observed climatology when driven by the corresponding observed boundary and initial conditions. The model performed satisfactorily in these experiments.

The MM4 has been used recently in many studies to simulate regional climate, see Giorgi.[14] The model is driven with output from a GCM; the high resolution of MM4 is utilized in resolving some physical effects which are not resolved by the GCM, e.g. effects of topography. This one-way nesting procedure can be very useful in making predictions about changes in the regional climate. These predictions are not usually possible using GCMs of coarse resolution. Implicit in this one-way nesting procedure is the assumption that the improvements or changes in description of the physical processes inside the model domain will not have any effect on the surrounding model atmosphere. This assumption is also relevant to our study.

2.3 The Biosphere–Atmosphere Transfer Scheme (BATS)

The land-surface is described as consisting of a vegetation layer, a surface soil layer, and a deep soil layer (root zone). A seasonally dependent fraction of the grid-cell area is covered with vegetation; the remaining fraction is assumed covered with bare soil. Soil temperature is predicted using a prognostic equation which corresponds to the force-restore method of Deardorff.[6] The temperatures of the canopy and that of the air within the canopy are determined using diagnostic equations which describe conservation of energy and conservation of water mass at the land-surface. The energy balance equation includes radiative, latent and sensible heat fluxes.

The land-surface hydrology scheme consists of prognostic water balance equations which predict the water content of the surface layer and of the root zone. The components of this water balance are rainfall, throughfall, infiltration, evapotranspiration, surface runoff, groundwater runoff, infiltration below root zone and diffusive exchange of water between the two layers. The soil water movement formulation is parametrized to fit the results of the simulations by Dickinson[7] using a high resolution soil model. It is assumed that the ratio of surface runoff to rainfall is equivalent to saturation in the surface soil layer raised to the fourth power. Saturation of the soil layer is defined as the ratio of the water depth in the soil layer to the maximum capacity of the layer.

The treatment of interception in BATS is rather simple. Whenever available canopy storage exceeds canopy storage capacity, drainage occurs with a rate which is directly proportional to excess canopy storage (the difference between available canopy storage and canopy storage capacity). Evaporation is a weighted average of transpiration by the plant and evaporation from the wet canopy. The effects of sub-grid scale spatial variability in rainfall or canopy storage are not included in this scheme. The results of previous modeling studies which used BATS, e.g. Dickinson and Henderson-Sellers,[9] suggest that the effects of spatial variability are important. Neglecting these effects results in over-estimation of interception loss.

The fluxes of latent heat, sensible heat and momentum are calculated using the similarity theory approach. The drag coefficients are calculated based on surface roughness and atmospheric stability of the surface layer. For neutral and stable conditions turbulent vertical transport is modeled using an eddy diffusion formulation. For unstable conditions transport is modeled by a dry convective adjustment scheme. BATS is described in detail by Dickinson et al.[3]

2.4 Modifications of the land-surface hydrology scheme

BATS includes a detailed description of the *vertical* structure of surface layer. In contrast, the scheme assumes constant surface properties and uniform forcing in the *horizontal*. Sub-grid scale spatial variability in rainfall, canopy storage and soil moisture play a significant role in some important processes taking place in a rain-forest environment. The partition of rainfall into throughfall and interception loss, and the subsequent partition of throughfall into infiltration and surface runoff are examples of these processes which are sensitive to the effects of sub-grid scale spatial variability. This sensitivity is basically due to the non-linearity involved in the interception and runoff processes. In this study, the BATS treatment of rainfall interception and runoff are modified to account for the effects of sub-grid scale spatial variability. These modifications are important because they balance the emphasis on *vertical* details by accounting for some of the important effects resulting from spatial variability in the *horizontal*.

A new rainfall interception scheme which accounts for the effects of spatial variability in rainfall and canopy storage is included into BATS. This scheme combines a physical description of rainfall interception given by the Rutter model[23] and statistical description of the sub-grid scale spatial variability in rainfall and canopy storage. A derived distribution approach is used to obtain expressions for the spatial average interception loss and canopy drainage. The details of the scheme are given in Eltahir and Bras.[12]

A runoff scheme similar to that of Entekhabi and

Eagleson[13] is developed for modeling surface runoff. It is assumed that the infiltration capacity of the top soil layer is linearly related to soil saturation of that layer. The spatial variability in rainfall and soil moisture are modeled using a statistical approach. Runoff occurs at any point where rainfall rate exceeds the infiltration capacity of the soil or where rainfall occurs on a saturated soil. Infiltration capacity is the maximum possible rate of infiltration into the soil layer. The runoff scheme is described in some detail by Eltahir.[10]

In accounting for the sub-grid scale spatial variability, it is assumed that rainfall occurs over a fraction of the total grid-cell area. Eltahir and Bras[11] provide a new formula for computing the fractional coverage of rainfall, μ. This formula is based on the observation that the average rainfall over the total area of the grid-cell (including wet and dry regions), divided by μ is a constant for a certain region and season of the year. This constant is equivalent to the climatological rainfall intensity. The new procedure for computing the fractional coverage of rainfall is consistent with observations of convective storms.

The modifications in modeling of rainfall interception, surface runoff, and the fractional coverage of rainfall are included, as part of BATS, into the climate model.

3 NUMERICAL EXPERIMENTS ON THE SENSITIVITY OF REGIONAL CLIMATE TO DEFORESTATION IN THE AMAZON

The MM4 is used in performing sensitivity experiments on the climate of the Amazon basin. The objective of these experiments is to study the effects of small-scale ($\sim$ 250 km) deforestation on the regional climate.
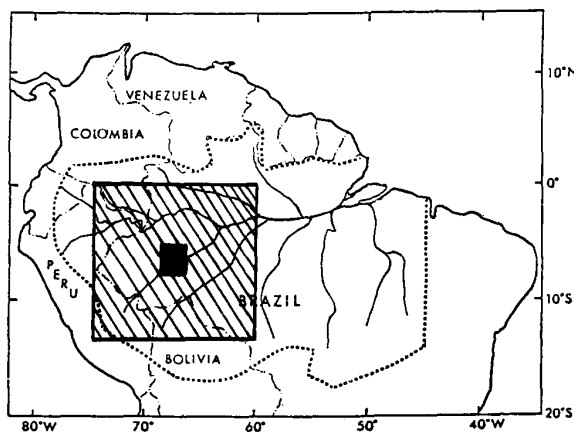
Table 1. Parameters of land cover and soil for rain-forest and short grass environments (after Dickinson et al.[8])

Parameter	Rain-forest	Short grass
Fractional vegetational cover	0·9	0·8
Roughness length (m)	2·0	0·02
Vegetation albedo for wavelengths $\geq 0\cdot7$ mm	0·2	0·3
Vegetation albedo for wavelengths $< 0\cdot7$ mm	0·04	0·10
Maximum leaf area index	6	2
Porosity	0·54	0·48
Saturated hydraulic conductivity (mm/s)	$3\cdot2\times10^{-3}$	$6\cdot3\times10^{-3}$

Fig. 2. The Amazon basin. The region of the numerical simulations is the hatched square; the deforested sub-region is the dark square.
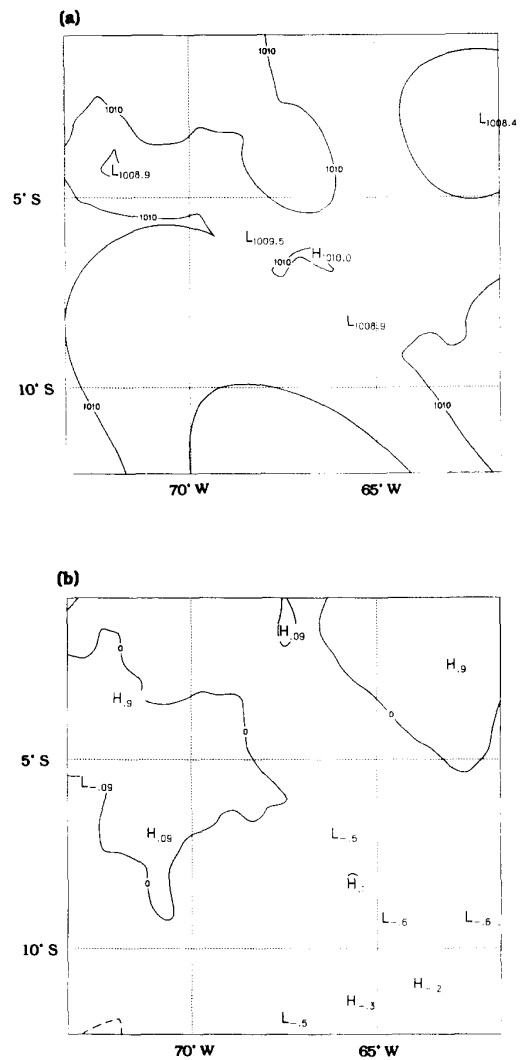

Fig. 3. Sea level pressure for January in mbar: (a) ECMWF data; (b) difference between the simulated field and the observed field.

3.1 Design of the experiments

The sub-region of the Amazon rain-forest considered in these experiments is centered at 6·5° S and 67·5° W, see Fig. 2. The scale of this region is 1600 km each side. The

sensitivity experiments are performed for the months of January and July to represent typical summer and winter conditions, respectively. For each of the two months, the experiment consists of two runs using the meso-scale climate model: a control run to simulate
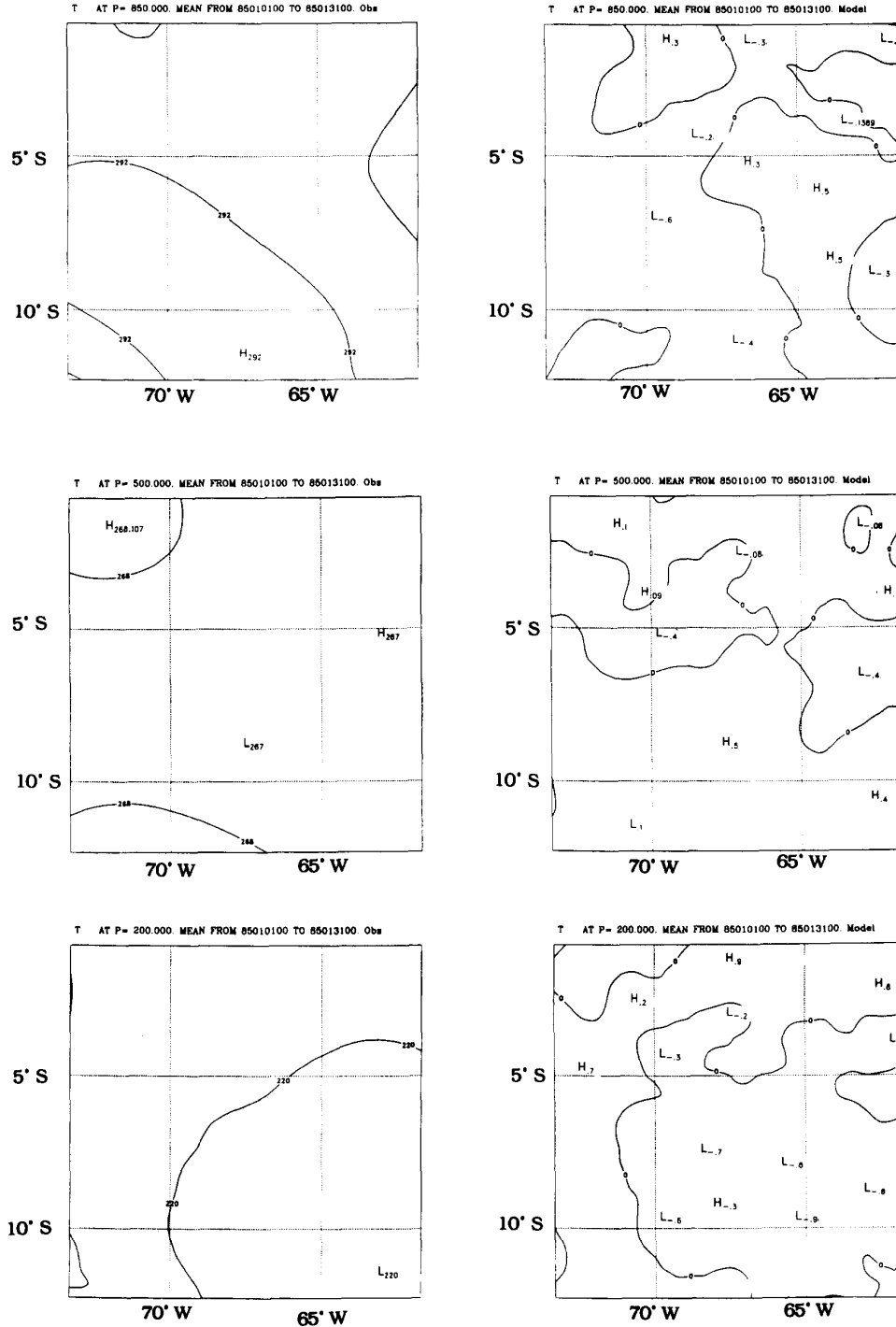

Fig. 4. Temperature in K for January. 'Obs' refers to ECMWF data and 'Model' refers to differences between the simulated fields and the observed fields.

the pre-deforestation state of the land–atmosphere system, and a perturbed run to simulate the post-deforestation state of the same system.

Deforestation is modeled by replacing the rain-forest with short grass in a region which is also centered at 6·5° S and 67·5° W but with a smaller scale of 250 km each side. The location of the deforested region is shown in Fig. 2. Deforestation is achieved in the model by changing the values of the parameters describing land cover and soil from those corresponding to rain-forest to the values corresponding to short grass. Some of these values are shown in Table 1.[8] The spatial resolution which is used in this study is 50 km in the horizontal. Fourteen pressure levels are distributed between the surface and the tropopause in the vertical. The temporal resolution is 90 s.

3.2 Boundary and initial conditions

The climates for January and July are simulated by driving the model with boundary conditions from assimilated data for January and July of the years 1985, 1986 and 1989. Since the years 1987 and 1988 include El Niño events, they are not included in these simulations. The control and perturbed climate states are estimated from the averages for January and July of the three years.

The climate model is driven by solar radiation and boundary conditions estimated from assimilated observations. The global data set assimilated by the European Centre for Medium-range Weather Forecast (ECMWF) is used in this study. The data used has a temporal resolution of twelve hours and a spatial resolution of
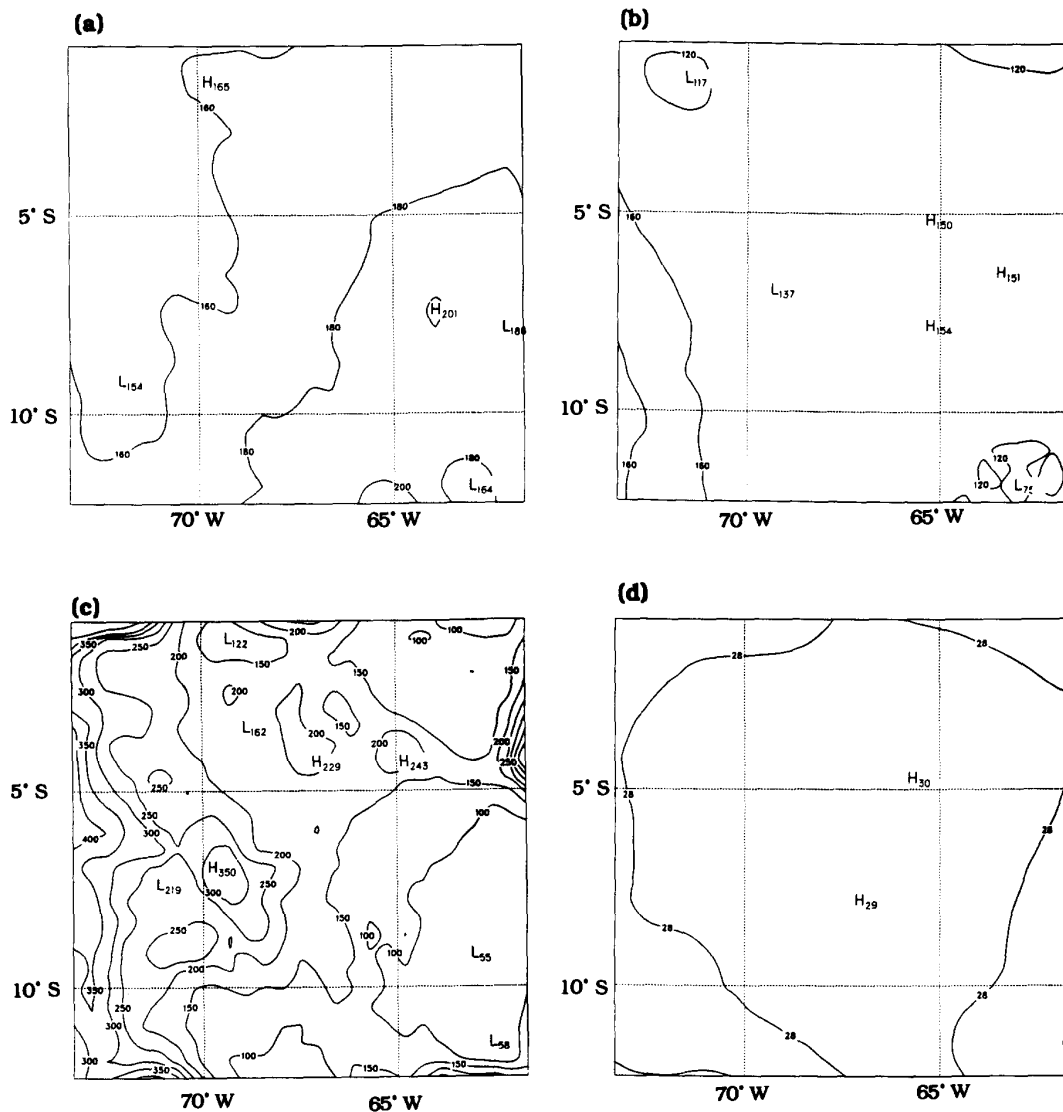

Fig. 5. (a) Net surface radiation in W/m^2; (b) evaporation in mm/month; (c) rainfall in mm/month; and (d) air temperature in °C. All variables for the month of January.

Table 2. Pre-deforestation climate in January (mm/month)

Variable	Model	Observations	References
Surface temperature	28·3°C	26·0°C*	(1)
Net surface radiation	178	120	(2)
Evaporation	140	107	(2)
Rainfall	184	270	(2)
Runoff ratio	47%	44%*	(3)

*Indicates that the observation is an annual value, see (1) Molion,[20] (2) Shuttleworth,[25] and (3) Oltman.[22]

Table 3. Sensitivity of regional climate to deforestation in the Amazon basin

Variable	Predicted change	
	January	July
Net surface radiation	−8%	−8%
Evaporation	−14%	−12%
Rainfall	−10%	−8%
Surface temperature	+0·6°C	+0·7°C

2·5°. These data values are interpolated linearly in space and time to match the resolutions of the MM4. Temperature and pressure are specified at the boundaries according to the ECMWF data. Wind and specific humidity are specified at the inflow boundaries from the

ECMWF analysis but the same two variables are predicted by the model solution at the outflow boundaries. Inflow boundaries are those where the component of the wind vector (which is estimated from
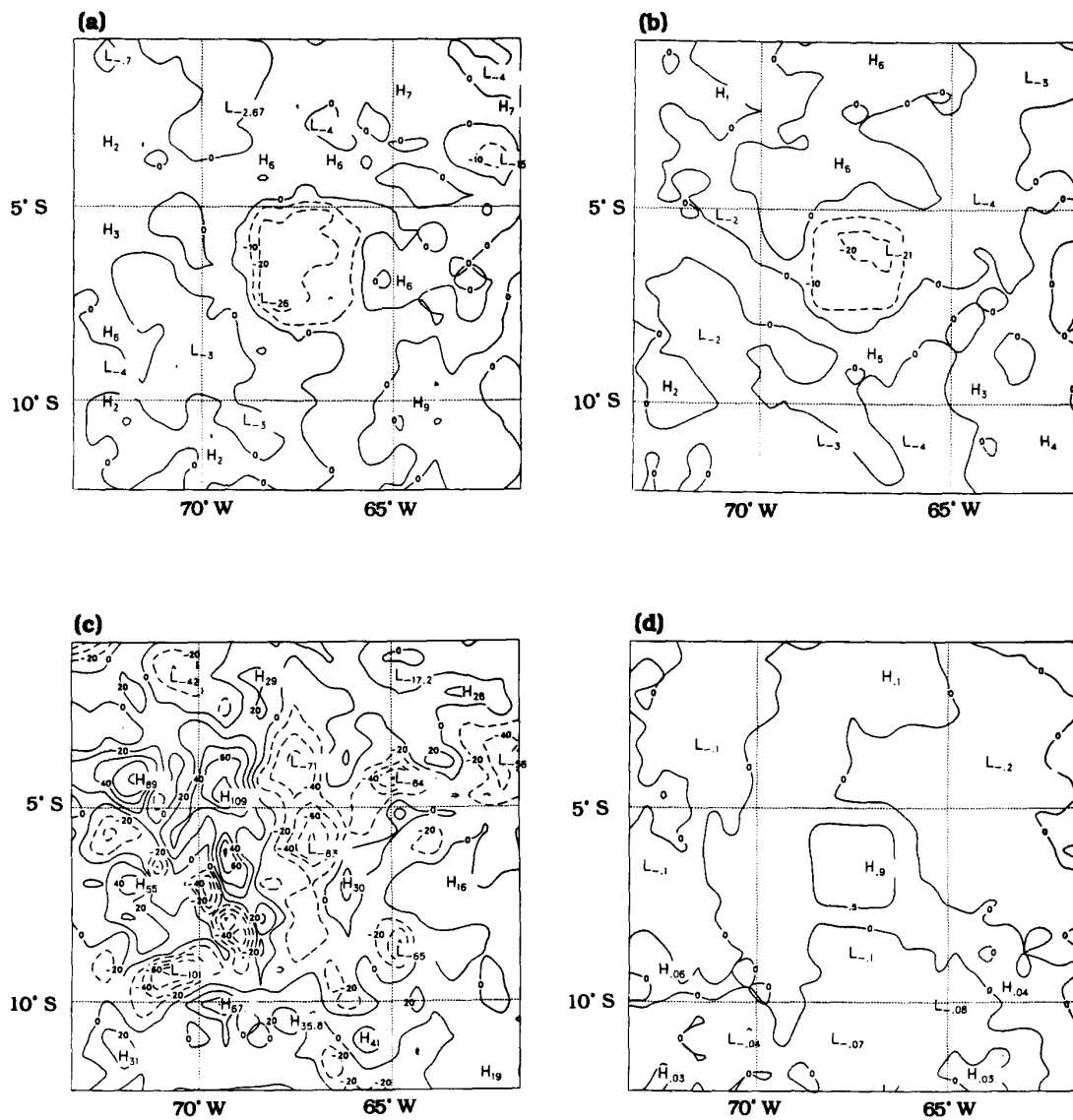

Fig. 6. Post-deforestation field minus (pre-deforestation field in January, for the following variables: (a) net surface radiation in W/m²; (b) evaporation in mm/month; (c) rainfall in mm/month; and (d) air temperature in °C.

the ECMWF data), perpendicular to the boundary, points into the domain of the simulation. Outflow boundaries are those where that same component points away from the domain of the simulation. The upper boundary condition is a no flow boundary.

The boundary conditions are specified in the manner described above in order to obtain a smooth solution with insignificant boundary effects. Specification of wind and specific humidity from the ECMWF data at all the boundaries may result in significant boundary effects (large gradients in some key variables such as rainfall near the boundaries).

For each month initial conditions are specified using the corresponding conditions from the ECMWF data. The initial soil moisture conditions are specified according to the standard values recommended by the original MM4 modeling system.[3] These values describe typical conditions for each season and land cover type.

3.3 Results for January

The results of the sensitivity experiment for January are presented in this section. The results of the control run and the perturbed run are presented separately. They describe the pre-deforestation and post-deforestation states of the land–atmosphere system as simulated by the climate model.

3.3.1 January climate: Pre-deforestation

The skill of the model in simulating the climate of the Amazon region in January is tested by comparing the fields for key atmospheric variables simulated by the model and the corresponding fields estimated from ECMWF data. Figures 3 and 4 show fields of sea level pressure and temperature (at 850 mbar, 500 mbar and 200 mbar) from the ECMWF data. The same figures show the differences between the fields simulated by the model and those from ECMWF data. The comparison indicates that the model is capable of reproducing the average climate of the region. A similar comparison is carried out for atmospheric water vapor with similar satisfactory results. The only exception is the upper troposphere where the amounts of water vapor are very small. Hence, although the error in simulating these amounts is small in absolute value, the relative error (in comparison to the water vapor amount) is significant.

In the following we focus on some variables which are important to the deforestation problem. Figure 5 shows the fields of net surface radiation, evaporation, surface temperature, and rainfall, which are simulated by the climate model for the pre-deforestation situation. Table 2 compares the spatial averages of some of these fields with observations. These comparisons are based on

surface observations from the region. Rainfall is underestimated by about 30%. This difference is large, but the accuracy of the model is reasonable when compared to the typical accuracy of climate models in predicting the distribution of rainfall. The large difference is due to underestimation of atmospheric moisture convergence into this sub-region by the ECMWF data. Underestimation of rainfall results in underestimation of cloudiness and for this reason overestimation of net surface radiation. The latter effect results in overestimation of evaporation. The model shows remarkable accuracy in predicting the runoff ratio in a rain-forest environment.

3.3.2 January climate: Post-deforestation

The sensitivity of regional climate in January to deforestation is measured by the differences between
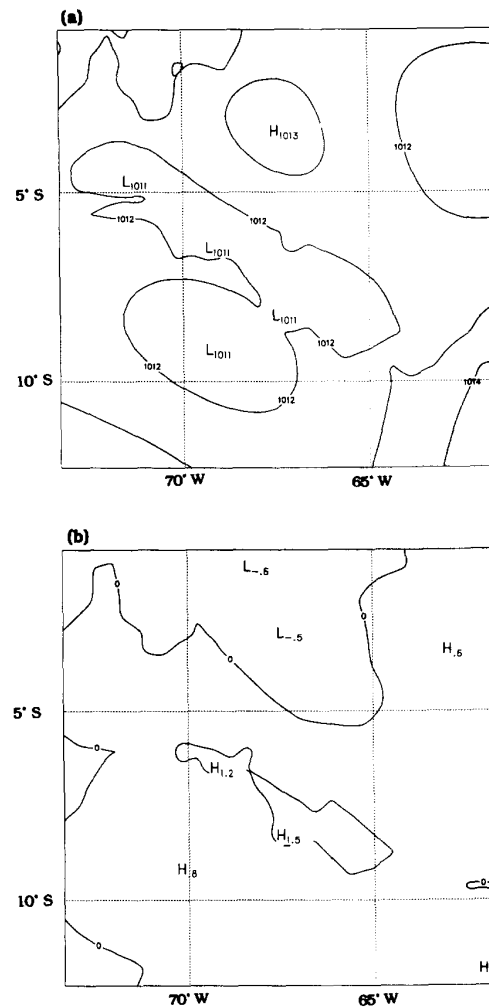
Fig. 7. Sea level pressure for July in mbar: (a) ECMWF data; (b) difference between the simulated field and the observed field.

the post-deforestation and the pre-deforestation fields of some key variables. Figure 6 shows the differences (post-deforestation minus pre-deforestation) for the variables: net surface radiation, evaporation, surface temperature, and rainfall. Table 3 presents the normalized differences between the post-deforestation and the pre-deforestation fields for the variables mentioned above, averaged over the deforested area. Deforestation results in less net surface radiation, less evaporation, less rainfall, and warmer surface temperature.
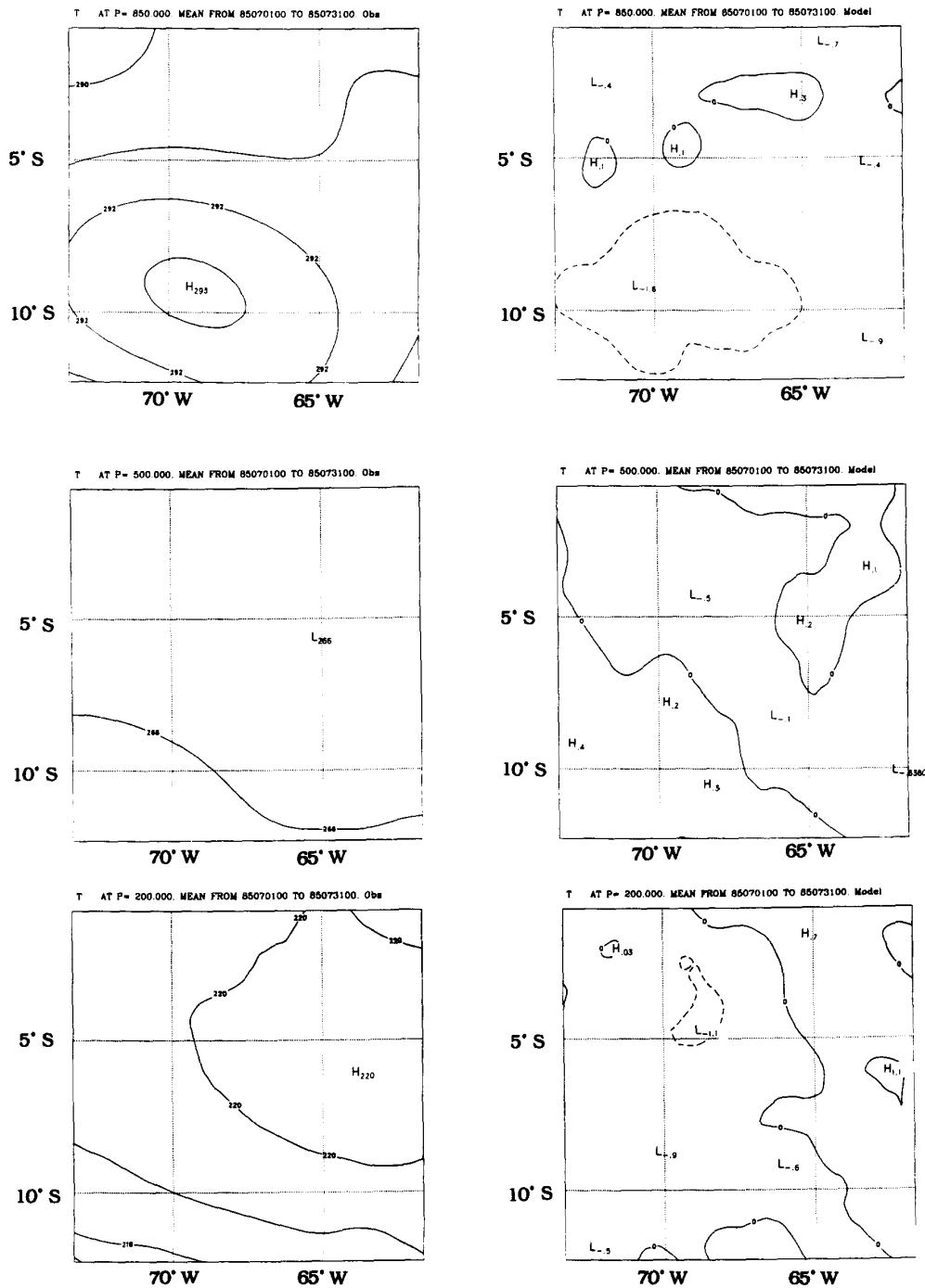

Fig. 8. Temperature in K for July 'Obs' refers to ECMWF data and 'Model' refers to differences between the simulated fields and the observed fields.
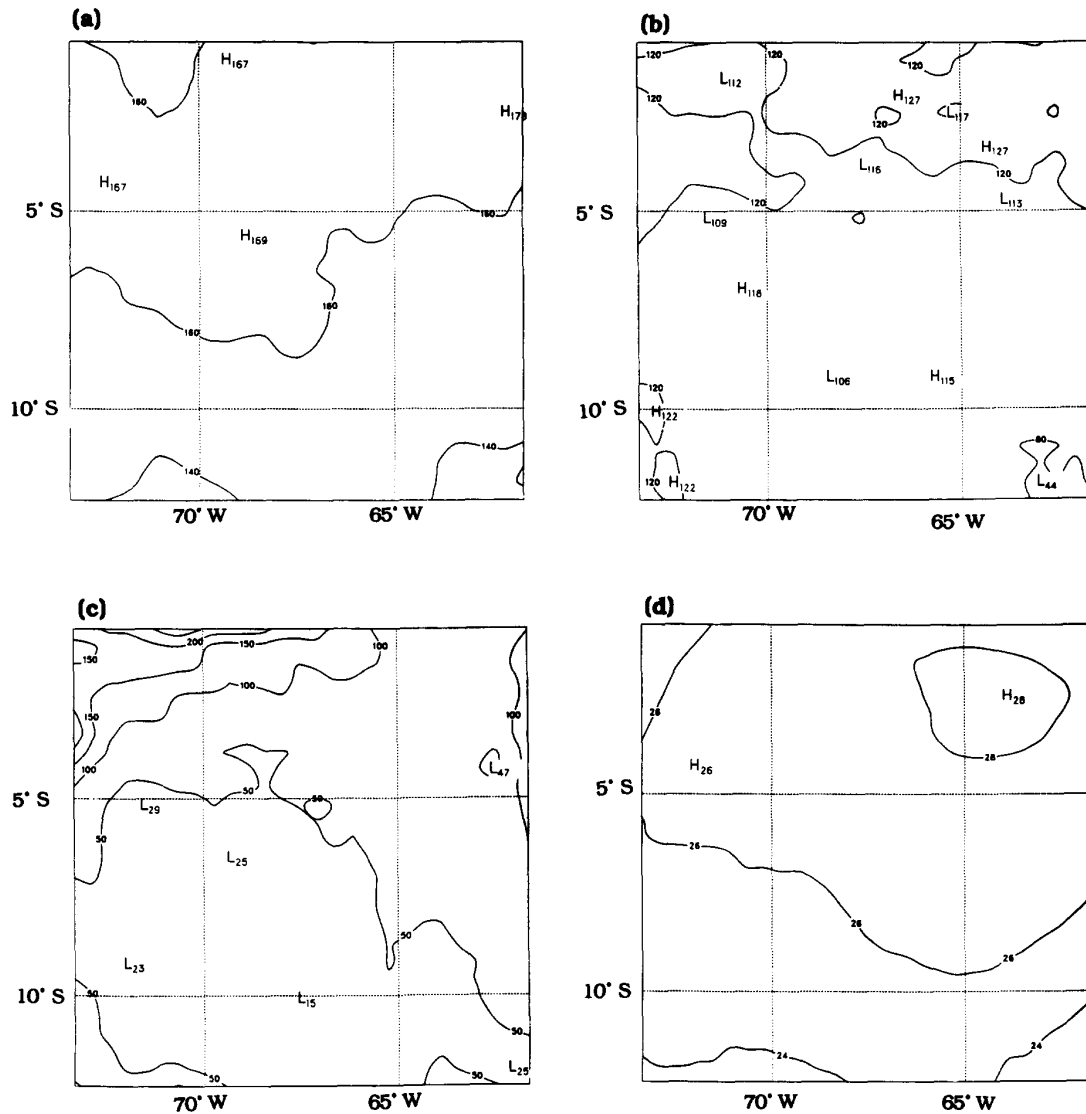
Fig. 9. (a) Net surface radiation in W/m^2; (b) evaporation in mm/month; (c) rainfall in mm/month; and (d) air temperature in °C. All variables for the month of July.

3.4 Results for July

This section is similar to Section 3.3, except that it presents results for the month of July.

3.4.1 July climate: Pre-deforestation

The ability of the model in simulating the climate of the Amazon region in July is tested by comparing the fields of some atmospheric variables simulated by the model and the corresponding fields from ECMWF data. Figures 7 and 8 show fields of sea level pressure and temperature (at 850 mbar, 500 mbar and 200 mbar) from the ECMWF data. The figures show the differences between the fields simulated by the model and those from ECMWF data. The comparison indicates that the

model is capable of reproducing the average climate of the troposphere. It is also found that the relative error in simulating water vapor amounts in the upper troposphere is significant, which is similar to the case of January.

Figure 9 shows the simulated fields of net surface

Table 4. Pre-deforestation climate in July (mm/month)

Variable	Model	Observations	References
Surface temperature	26·2°C	26·0°C*	(1)
Net surface radiation	165	131	(2)
Evaporation	115	119	(2)
Rainfall	64	110	(2)
Runoff ratio	42%	44%*	(3)

*Indicates that the observation is an annual value. References describing observations are indexed in Table 2.
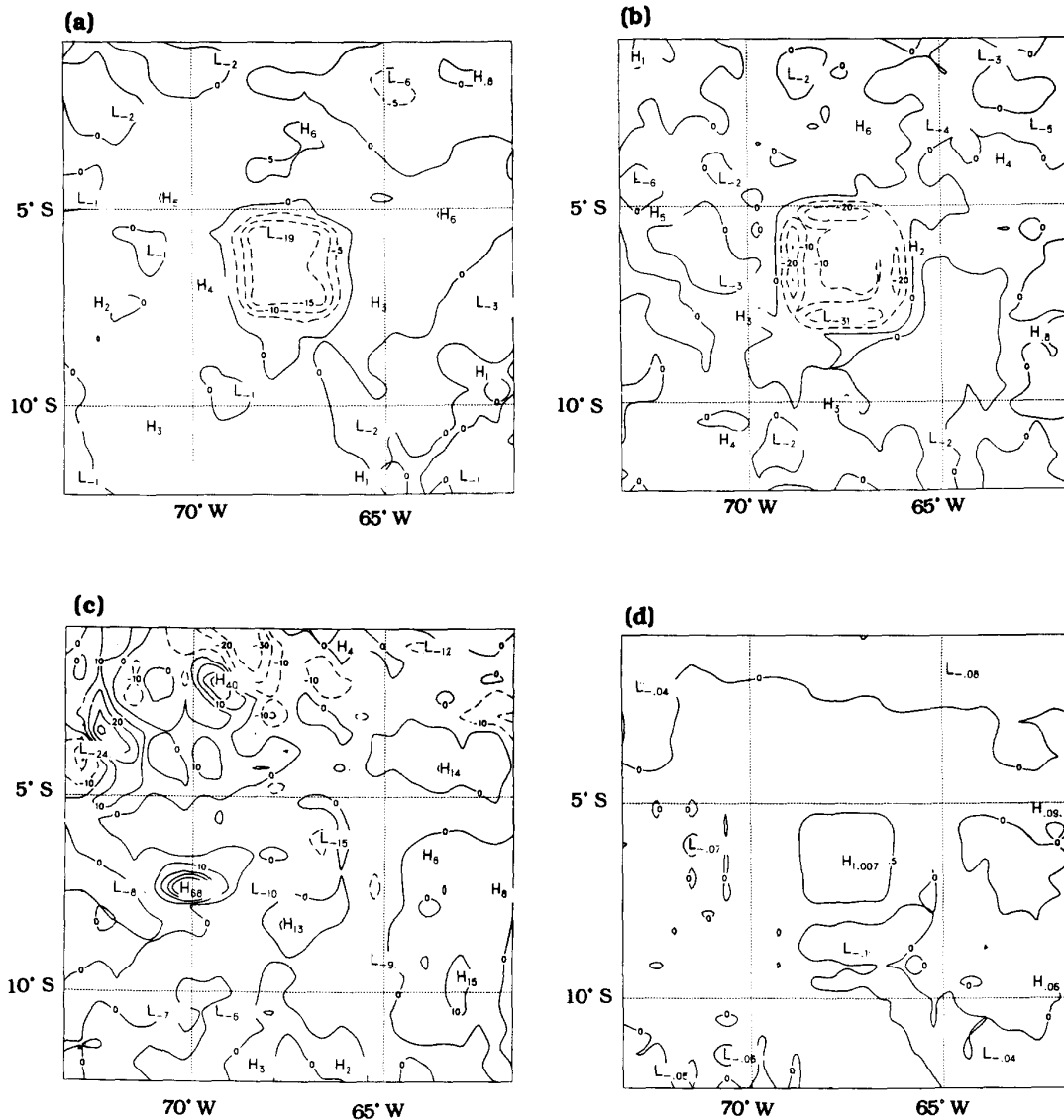
Fig. 10. Post-deforestation field minus pre-deforestation field in July, for the following variables: (a) net surface radiation in W/m^2; (b) evaporation in mm/month; (c) rainfall in mm/month; and (d) air temperature in °C.

radiation, evaporation, surface temperature and rainfall. Table 4 compares the spatial averages of some of these fields with surface observations from various sources. It shows similar features as those in Table 2, namely underestimation of rainfall and cloudiness and overestimation of net surface radiation. Evaporation and runoff ratio are accurately predicted by the model.

3.4.2 July climate: Post-deforestation

The sensitivity of regional climate in July to deforestation of the small area located in the center of the region is measured by the differences between the post-deforestation and the pre-deforestation fields for some key variables. Figure 10 shows these differences (post-deforestation minus pre-deforestation) for the

variables: net surface radiation, evaporation, surface temperature, and rainfall. Table 3 presents the normalized differences between the post-deforestation and the pre-deforestation fields for the variables mentioned above, averaged over the deforested area. The relative changes in evaporation and rainfall are similar to those in the simulations for January, but the absolute values of these changes are different.

4 COMPARISON OF THE RESULTS OF NUMERICAL AND FIELD EXPERIMENTS

During the last decade several field experiments have been carried out in the Amazon region. The Amazon

Table 5. Comparison of simulations and observations of the partition of net surface radiation and rainfall by the rainforest

Variable	January		July	
	Model	Obs.	Model	Obs.
Evaporation/ (net surface radiation)	79%	89%	70%	91%
(Interception loss)/rainfall	12%	10%	14%	20%

Region Micro-meteorological Experiment (ARME) took place in the period September 1983–September 1985 over undisturbed tropical rain-forest. The site of this experiment (Reserve Ducke) is located 25 km northwest of Manaus in the Central Amazon basin. The objective of the experiment was to collect hydrological data about the rain-forest which can be used in calibrating climate models.

In the following, we focus on two processes: the partition of net radiation into latent and sensible heat fluxes, and the partition of rainfall into interception loss and throughfall. These two processes represent some of the important ways by which the rain-forest influences land-surface hydrology. Some of the results of ARME are shown in Table 5. The results are presented as ratios of the relevant forcing. The reason for presenting the results in this form is to separate the effects that are attributable to the land-surface scheme from those which are related to other components of the model. The observations in Table 5 indicate that about 90% of net surface radiation is utilized by the efficient evapotranspiration process from the rain-forest. The model simulates a smaller ratio of about 75%. This difference can be explained, at least partly, by underestimation of rainfall in the model simulations. This latter effect results in drier soil moisture conditions, implying that less water is available for evapotranspiration. The observations of normalized interception loss compare reasonably well with the results of the simulations. Previous modeling studies on the Amazon deforestation problem included significant errors (factors of two or three) in modeling of rainfall interception, see Lean and Warrilow,[19] Dickinson and Henderson-Sellers.[9] The comparison in Table 5 reveals that significant improvements in modeling of rainfall interception are achieved by including the effects of sub-grid scale spatial variability in rainfall and canopy storage.

In a recent paper, Bastable et al.[5] presented the first comparative observations of the micro-meteorology over cleared and undisturbed forest in the Amazon region. The undisturbed forest site (Reserve Ducke) is the same site used during ARME. The cleared forest site (Fazenda Dimona) is a cattle ranch which is located 100 km north of Manaus. The observations consist of a continuous 60 days of data from the middle of October 1990 to the middle of December 1990. The data were
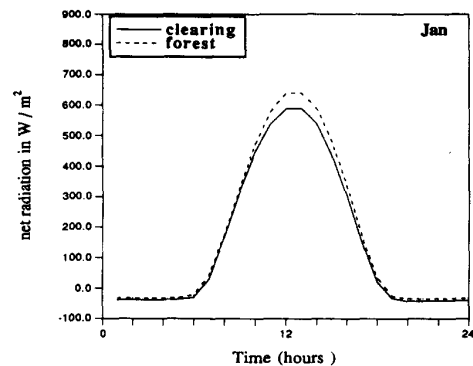
collected at the two sites simultaneously. Since the effects due to deforestation occur mainly through the changes in the surface energy balance, the following comparison focuses on that balance.
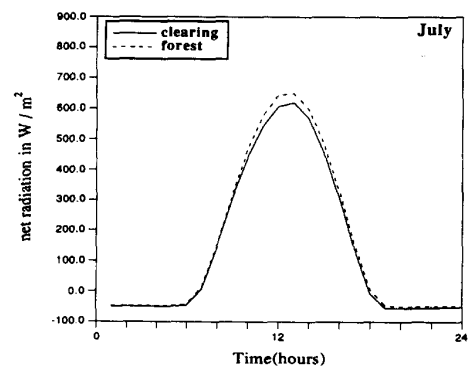
The net surface radiation measured at the two sites
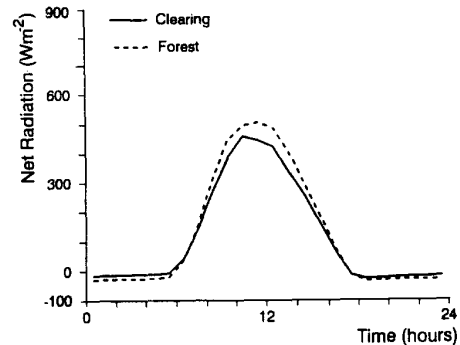
Fig. 11. Net surface radiation in W/m². (a) Observations, mid-October to mid-December of 1990, from Bastable et al.[5]; (b) model simulations, averaged for cleared and undisturbed forest, for January; (c) model simulations, averaged for cleared and undisturbed forest, for July.
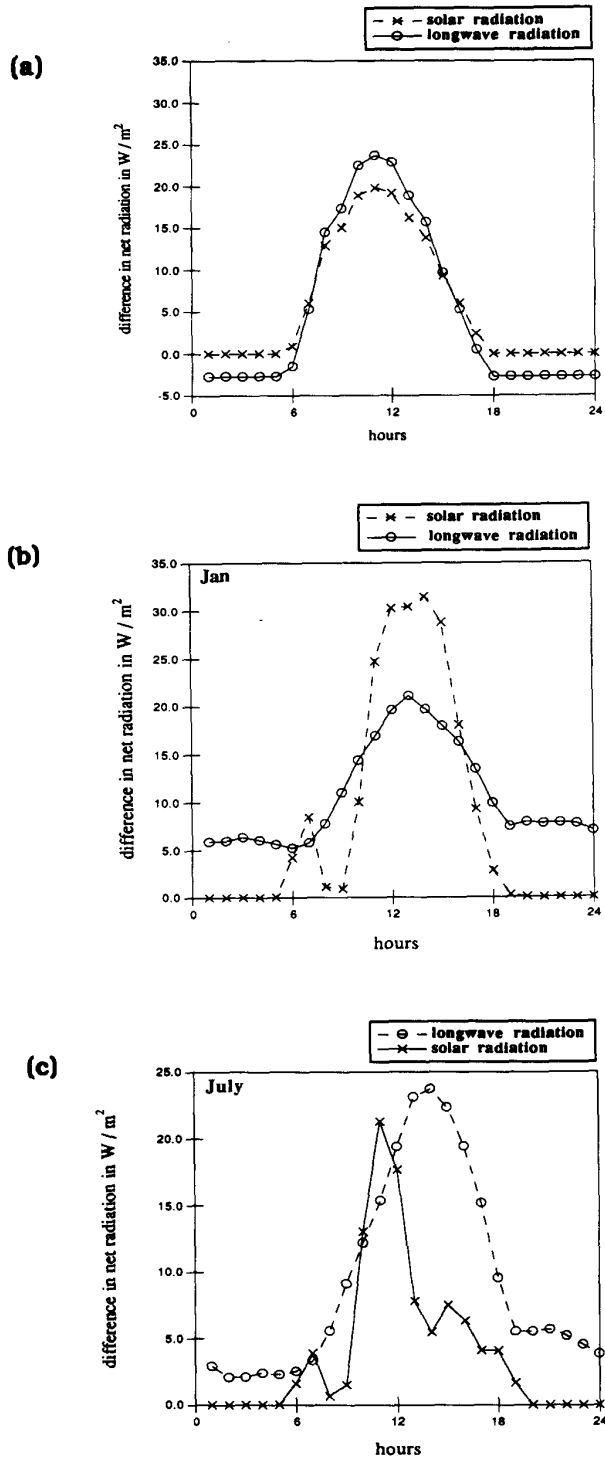
(a)

(b)

(c)

Fig. 12. Components of the difference in net surface radiation. (a) Observations, mid-October to mid-December of 1990, reproduced from the results Bastable *et al.*[5]; (b) Model simulations, January; (c) model simulations, July. The observations in (a) are computed from measurements of surface solar radiation and correlations of each of the two components of net radiation with solar radiation. The simulations in (b) and (c) are computed from the averages of each of the two components of net surface radiation over cleared and undisturbed forest.

and averaged for the 60 day period is shown in Fig. 11. The net surface radiation at the cleared site is less than net radiation above the forest. The same figure shows the simulated net surface radiation averaged over the undisturbed forest and the cleared area of the model domain. Although the model overestimates the net surface radiation, the observations and the simulations agree in the sign and order of magnitude of the difference in net surface radiation.

Net surface radiation has two components: net solar radiation which is equivalent to incident solar radiation minus reflected solar radiation, and net long-wave radiation which is equivalent to downwards flux of long-wave radiation minus upwards flux of long-wave radiation. Figure 12 shows these two components from observations and model simulations. These figures suggest that the differences in net surface radiation between the forest and cleared sites is contributed to, almost equally, by both components: solar radiation and long-wave radiation. Hence, the changes to the surface energy balance caused by deforestation are reflected on surface radiation at both short and long waves. This conclusion is confirmed by the observations as well as the model simulations.

The observations in Fig. 12(a) indicate that night-time long-wave radiation is slightly larger at the cleared site as compared to the forest. The magnitude of this difference is of the order of $-2\,\mathrm{W/m^2}$. In contrast, the model simulations which are shown in Figs 12(a), (b) and (c) show a decrease in night-time net long-wave radiation. The disagreement between the model and observations in this aspect of the change in surface radiation points to the limits on the accuracy of the model in simulating radiation processes.

5 DISCUSSION AND CONCLUSIONS

In this study, surface hydrology is simulated with reasonable accuracy. As presented in Tables 2, 4, and 5, the surface runoff ratio and the interception ratio simulated by the model are close to the observed values. This accuracy indicates that our modifications of BATS represent significant improvements. These modifications include the physical–statistical representation of rainfall interception and surface runoff and the new formula for computing the fractional coverage of rainfall.

The results presented in this paper suggest that small-scale ($\sim 250\,\mathrm{km}$) deforestation is likely to result in the following changes over the deforested area: less net surface radiation, less evaporation, less rainfall and warmer surface temperature. The predicted changes vary in absolute magnitude between summer and winter but the relative changes are of similar magnitudes. The rainfall changes are about -9% ($\pm 5\%$) and the evaporation changes are -13% ($\pm 5\%$). The change in surface temperature is about $+0.6^{\circ}\mathrm{C}$ ($\pm 0.5^{\circ}\mathrm{C}$).

Previous modeling studies,[19,21] predict that large-scale (~ 2500 km) deforestation in the Amazon basin is likely to result in the following effects: less evaporation, less rainfall, and warmer surface temperature. The magnitudes of the changes in evaporation and rainfall are of the order of 20 to 30%, the magnitude of the change in surface temperature is of the order of 2°C. The predicted changes due to small-scale deforestation are smaller than those due to large-scale deforestation by about a factor of 2. Possible reasons for this difference include the effects of the boundaries, since boundary to area ratio is larger for the smaller regions. The boundary effects can be seen in the figures which show the changes due to deforestation increasing from the boundary to the interior of the deforested region. Another important factor is the lower recycling ratio for smaller scales. The recycling ratio quantifies the relative contribution of local evaporation to local rainfall. The dependence of the recycling ratio in the Amazon on the scale considered is quantified by Eltahir;[10] as the scale of the region considered decreases the potential for interactions between hydrology and climate decreases.

The predicted magnitudes of the changes due to small-scale (~ 250 km) deforestation are comparable to the accuracy in the measurements of the variables involved. These changes are also comparable in magnitude to the natural spatial variability of the same variables. Hence, it would be difficult to detect the changes due to deforestation from field observations. The spatial distribution of the predicted changes due to deforestation indicates that the maximum changes are likely to occur near the center of the deforested region. This information can be utilized in field experiments which are designed for detection of the effects of deforestation using observations of surface temperature, evaporation, and rainfall. Long records of simultaneous observations on these key variables at two sites are necessary for detecting the effects of deforestation; one site should be located in the forest and the other located in the deforested area. Both sites should be located away from the boundary between the two regions.

Except for the rainfall changes, the predictions about the effects of deforestation are limited to the deforested area. Positive and negative rainfall changes of comparable magnitude occur over a larger area. Since the climates for January and July are estimated from only three months of simulations, it would be difficult to conclude if the changes in the rainfall field have any physical significance or if these changes are due to the sampling error.

The sensitivity results are interpreted as follows: deforestation results in less absorption of solar radiation at the surface and as a result the net radiation at the surface is reduced over the deforested region. Another important effect is the shorter roughness length of the deforested area; this effect reduces the eddy transport of heat and water vapor near the surface. The reduction of net radiation combined with the reduction in the efficiency of the eddy transport mechanism result in less evaporation from the deforested area. The reduction in evaporation results in less evaporative cooling at the surface and that explains the warming of surface temperature. The reduction in evaporation results in a drier boundary layer, limits the supply of water vapor, and that in effect, reduces the energy available for convection and rainfall. Other secondary feedbacks and effects follow deforestation. The reduction in net long-wave radiation is an example of these effects.

The model simulations agree with the recent observations of Bastable et al.[5] about the different components of the surface energy balance over cleared and undisturbed forest. Net surface radiation over cleared areas is less than that over undisturbed sites. This difference in net surface radiation is equally attributable to both of its components: solar radiation and long-wave radiation. It is suggested that deforestation introduces changes of comparable magnitudes in all the components of the surface energy balance. These changes are not limited to the increase in surface albedo as assumed by the traditional approaches to this problem.

The differences in the two components of net radiation can be explained as follows: as a result of deforestation some of the bio-mass which used to absorb solar radiation is removed. This direct effect results in larger surface albedo and reduces net solar radiation. The change in net long-wave radiation is less obvious. Three factors possibly contribute to modifying the long-wave radiation pattern. The warming of surface temperatures increases the emission of upward long-wave radiation by the surface implying a reduction in net long-wave radiation. Another important factor is the drying of the boundary layer following deforestation; it results in reducing absorption (trapping) of outgoing long-wave radiation and hence reduces net surface long-wave radiation. The physics of this drying effect is similar to that of the green-house problem. The third factor is the reduction in convection, cloudiness, and rainfall which follow deforestation. Less cloudiness results in less downward long-wave radiation and more outgoing long-wave radiation. Both of these effects result in reducing net long-wave radiation. Determination of the relative contributions of these three factors (or the possibility of other factors) will remain a subject for future research.

In the numerical simulations which are described in this paper, the size of the deforested area (~ 250 km) is small compared to the equatorial Rossby radius of deformation (~ 1000 km) which defines the physical scale for dynamics in the tropical atmosphere. Hence, the changes in regional climate due to small-scale deforestation are not likely to excite any response which may alter the large-scale circulation in the tropics. If that is true then the one-way nesting

procedure is accurate enough for studying deforestation at this scale. A more serious concern about this one-way nesting procedure is the constraint imposed on surface hydrology by fixing the amount of atmospheric moisture convergence. Any changes in the surface hydrology of the interior domain is constrained by the requirement that it should result in a fixed amount of atmospheric moisture convergence. The latter is predetermined by the boundary conditions. This comment is relevant to all climate studies which use the one-way nesting procedure.

ACKNOWLEDGEMENTS

REFERENCES

1. Anthes, R. A. A cumulus parametrization scheme utilizing a one-dimensional cloud model. *Mon. Weather Rev.*, **106**, (1977) 1045–78.
2. Anthes, R. A. Recent applications of the Penn. state/ NCAR meso-scale model to synoptic, meso-scale and regional climate studies. *Bull. Amer. Meteorol. Soc.*, **71** (1990) 1610–29.
3. Anthes, R. A., Hsie, E. Y. & Kuo, Y. H. Description of the Penn. state/NCAR meso-scale model version 4 (MM4). *NCAR Tech. Note, NCAR/TN-282+STR.* NCAR, Boulder, Colorado, 1987, 66 pp.
4. Anthes, R. A., Kuo, Y.-H., Hsie, E. Y., Low-Nam, S. & Bettge, T. W. Estimation of skill and uncertainty in regional numerical models, *Quart, J. Roy. Meteorol. Soc.*, **115** (1989) 763–806.
5. Bastable, H. G., Shuttleworth, W. J., Dallarosa, R. L. G., Fisch, G. & Nobre, C. A. Observations of climate, albedo and surface radiation over cleared and undisturbed Amazonian forest. *Int. J. Climatol.*, **13** (1993) 783–96.
6. Deardorff, J. W. Parametrization of the planetary boundary layer for use in general circulation models. *Mon. Weather Rev.*, **100** (1972) 93–106.
7. Dickinson, R. E. Modeling evaportranspiration for three-dimensional global climate models. In *Climate Processes and Climate Sensitivity*, eds J. E. Hansen & T. Takahashi American Geophysical Union, Washington, DC, 1984, pp. 58–72.
8. Dickinson, R. E., Henderson-Sellers, A., Kennedy, P. J. & Wilson, M. F. Biosphere–Atmosphere Transfer Scheme (BATS) for the NCAR community climate model. *NCAR Tech. Note, NCAR/TN-275+STR.* Boulder, Colorado, 1986, 69 pp.
9. Dickinson, R. E. & Henderson-Sellers, A. Modeling tropical deforestation: a study of GCM land surface parametrizations. *Quart. J. Roy. Meteorol. Soc.*, **144** (1988) 439–62.
10. Eltahir, E. A. B. Interactions of hydrology and climate in the Amazon basin. Doctorate Thesis, Department of Civil and Environmental Engineering, Massachusetts Institute of Technology, Cambridge, Massachusetts, 1993, pp. 188.
11. Eltahir, E. A. B. & Bras, R. L. On the estimation of the fractional coverage of rainfall in climate models. *J. Climate*, **6** (1993) 639–44.
12. Eltahir, E. A. B. & Bras, R. L. A description of rainfall interception over large areas. *J. Climate*, **6** (1993) 1002–8.
13. Entekhabi, D. & Eagleson, P. S. Landsurface hydrology parametrization for atmospheric general circulation models including subgrid scale spatial variability. *J. Climate*, **2** (1989) 816–31.
14. Giorgi, F. Simulation of regional climate using a limited area model nested in a general circulation model. *J. Climate*, **3** (1990) 941–63.
15. Giorgi, F. & Bates, G. T. The climatological skill of a regional model over complex terrain. *Mon. Weather Rev.*, **117** (1989) 2325–47.
16. Harris, R. C., Wofsy, S. C., Garstang, M., Browell, E. V., Molion, L. C. B., McNeal, R. J., Hoell Jr, J. M., Bendura, R. J., Beck, S. M., Navaro, R. L., Riley, J. T. & Snell, R. L. The Amazon Boundary Layer Experiment (ABLE 2A) dry season 1985. *J. Geophys. Res.*, **93** (D2) (1988) 1351–60.
17. Houghton, R. A. Tropical deforestation and atmospheric carbon dioxide. *Climatic Change*, **19** (1991) 99–118.
18. Lacis, A. A. & Hansen, J. E. A parametrization for the absorption of solar radiation in the Earth's atmosphere. *J. Atmos. Sci.*, **31** (1974) 118–33.
19. Lean, J. & Warrilow, D. A. Simulation of the regional climatic impact of Amazon deforestation. *Nature*, **342** (1989) 411–13.
20. Molion, L. C. B. A climatonomic study of the energy and moisture fluxes of the Amazons basin with considerations of deforestation effects. PhD Thesis, University of Wisconsin, Madison, 1975, 132 pp.
21. Nobre, C. A., Sellers, P. J. & Shukla, J. Amazonian deforestation and regional climatic change. *J. Climate*, **4** (1991) 957–88.
22. Oltman, R. E. Reconnaissance investigation of the discharge and water quality of the Amazon. *Biota Amazonica*, **3** (1967) 163–85.
23. Rutter, A. J., Kershaw, K. A., Robins, P. C. & Morton, A. J. A predictive model of rainfall interception in forests. I. Derivation of the model from observations in a plantation of Corsican pine. *Agric. Meteorol.*, **9** (1971) 367–84.
24. Shuttleworth, W. J. Evaporation from Amazonian rainforest. *Phil. Trans. R. Soc. Lond.*, **B233** (1988) 321–46.
25. Shuttleworth, W. J. Macrohydrology — the new challenge for process hydrology. *J. Hydrol.*, **100** (1988) 31–56.
26. Shuttleworth, W. J., Gash, J. H. C., Roberts, J. M., Nobre, C. A., Molion, L. C. B. & Ribeiro, N. M. G. Post-deforestation Amazonian climate: Anglo-Brazilian research to improve prediction. *J. Hydrol.*, **129** (1991) 71–86.